Regenerative Therapy 28 (2025) 431–437

Contents lists available at ScienceDirect

Regenerative Therapy

journal homepage: http://www.elsevier.com/locate/reth

Original Article

Applicability of the regression approach for histological multi-class grading in clear cell renal cell carcinoma

Mayu Shibata [a, b], Akihiro Umezawa [a, *], Saki Aoto [c], Kohji Okamura [d], Michiyo Nasu [a], Ryuichi Mizuno [e], Mototsugu Oya [e], Kei Yura [b, f, g], Shuji Mikami [h]

[a] Center for Regenerative Medicine, National Center for Child Health and Development Research Institute, Tokyo, Japan
[b] Department of Transdisciplinary Engineering, Ochanomizu University, Tokyo, Japan
[c] Medical Genome Center, National Center for Child Health and Development Research Institute, Tokyo, Japan
[d] Department of Systems BioMedicine, National Center for Child Health and Development Research Institute, Tokyo, Japan
[e] Department of Urology, Keio University School of Medicine, Tokyo, Japan
[f] Center for Interdisciplinary AI and Data Science, Ochanomizu University, Tokyo, Japan
[g] Graduate School of Advanced Science and Engineering, Waseda University, Tokyo, Japan
[h] Department of Pathology, Keio University School of Medicine, Tokyo, Japan

A R T I C L E I N F O

Article history:
Received 5 October 2024
Received in revised form
23 December 2024
Accepted 10 January 2025

Keywords:
Carcinoma grading
Classification models
Regression models
Intra-tumor heterogeneity (ITH)
Convolutional neural networks (CNN)

A B S T R A C T

The histological grading of carcinoma has been one of the central applications of task-specific deep learning in pathology. The deep learning method has pushed away the regression approach, which has been exploited for two-class classification, to address multi-class classification. However, the applicability of the regression approach on multi-class carcinoma grading has not been extensively investigated. Here, we show that the regression approach is sufficiently compatible with classification regarding the four-class grading of clear cell renal cell carcinoma using 11,826 histological image patches from 16 whole slide images. Using convolutional neural network models (DenseNet-121 and Inception-v3), we found that regression models predict as accurately as classification models, achieving an accuracy of 0.990 at the highest, with fewer prediction errors by two or more grades. Furthermore, we found that the predictions by the regression models qualitatively capture intra-tumor heterogeneity of grades using the composite image patches. Our results demonstrate that the regression approach offers advantages in making a core of the multi-class grade prediction tools for practice.

1. Introduction

Carcinoma grading on histopathological images has been one of the central applications of task-specific deep-learning techniques in pathology today. These studies stretch across a wide range of cancers/tumors, including the well-studied organs, such as brain [1,2], breast [3–5], and prostate [6,7]. The simplest form of the grading problems is the binary classification. This type of problem comprises malignant/benign classification of colon cancer [8] and breast cancer [9], and low/high-grade classification of clear cell renal cell carcinoma (ccRCC) [10]. Some of these problems were addressed by machine learning models performing regression. Although regression is widely recognized as one of the established approaches to address histological binary classification, the approach loses its presence in multi-class grading problems. For such problems, the classification approach is taken almost dominantly, as can be seen in the studies, including three-class grading of oral squamous cell carcinoma [11], five-class Gleason grading of prostate cancer [12], and four-class grading of brain tumor [1]. However, the applicability of the regression approach on histological multi-class carcinoma grading has not been extensively examined. It is possible that the regression machine learning models attain higher predictive performance than classification models, because they retain the relations among the carcinoma grades which often correspond with the progression and/or

* Corresponding author. Center for Regenerative Medicine, National Center for Child Health and Development Research Institute, 2-10-1 Okura, Setagaya, Tokyo, 157-8535, Japan.
E-mail address: umezawa-a@ncchd.go.jp (A. Umezawa).
Peer review under responsibility of the Japanese Society for Regenerative Medicine.

https://doi.org/10.1016/j.reth.2025.01.011

prognosis. Despite the pathological importance of such information, it is usually lost in the multi-class classification, which is implemented in a one-vs-rest manner [13].

Additionally, the regression approach is expected to offer a unique advantage on carcinoma grade prediction, *i.e.* the detection of intra-tumor heterogeneity (ITH). ITH refers to the heterogeneity within the tumor of a single case ranging from genomic to phenotypic level, including carcinoma grades [14]. ITH is known to be closely related to the progression, prognosis, and treatment outcomes [14,15]. Therefore, its detection is vital for understanding the biomedical conditions of the patients and planning effective treatments accordingly. If the detection capability of the regression models on ITH is proven, they can be implemented in the grading supportive tools for practice. Such tools enable efficient and ITH-sensitive grading without any time- and labor-expensive additional experiments/procedures. In this study, we examine the predictive performance of the regression models on the histological multi-class grading problem and ITH detection of carcinoma, taking ccRCC as an example.

ccRCC is the most prevalent subtype of renal cell carcinoma that develops from renal epithelia [16–18]. Carcinoma of this subtype is known by the aggressive phenotype and poor prognosis [17,19,20]. Histologically, ccRCC is categorized into one of the four grades, namely grade 1 (G1) to grade 4 (G4), according to the World Health Organization/International Society of Urological Pathology (WHO/ISUP) histological grading of renal cell tumors [21,22]. According to this criterion, G1 to G3 are graded by the nucleolar prominence; nucleoli are unobtrusive and distinct under 400-fold magnification in G1 and G2 tumors, respectively, and they are conspicuous under 100-fold magnification in G3 tumors. G4 is characterized by atypical nuclear pleomorphism and/or sarcomatoid or rhabdoid differentiation. This grading is validated to be prognostically significant [23]. Notably, ccRCC is well known for the formation of the ITH [24–28]. The established multi-class grading system and formation of the ITH make ccRCC suitable for evaluating the predictive performance of the regression models in this study.

In this work, we developed convolutional neural network (CNN) models for the four-class histopathological grading of ccRCC to examine the applicability of the regression approach on multi-class carcinoma grading. Furthermore, we analyzed the applicability of our regression models on ITH utilizing composite images mimicking ITH. Our results cast light on the advantages regression models offer in predicting histological multi-class grading of carcinoma. This study will promote the use of the regression approach for a practical carcinoma grading tools to support medical practitioners for more efficient and accurate grading.

2. Results and discussion

2.1. Image patches

After selecting whole slide images (WSIs) of uniform grade, four WSIs were randomly sampled for each grade for further analyses to balance the amount of data among the grades (Table 1). The limited number of WSI images was intentionally chosen to demonstrate the conceptual applicability of regression models in multi-class grading rather than creating a clinical diagnostic tool. We adopted the widely used image patch approach [29–31] in this study. From the manually annotated carcinoma region on these WSIs, patches with a side of approximately 200 μm were randomly segmented. The size of the patches was determined as the minimal area required for reliable grade diagnosis, empirically deduced from our observations, including experienced pathologists. To minimize the load of the data annotation, a total of 11,826 patches were labeled following the grades given to the individual WSI they were segmented from (Fig. 1). To complement the insufficiency of the training data, the patches of G3 and G4 were augmented as described in MATERIALS AND METHODS section.

Table 1
Number of WSIs and image patches.

Grade	The WSIs of uniform grade	The WSIs used for analyses	Image patches
1	4	4	3,521
2	63	4	3,305
3	35	4	2,328
4	4	4	2,672

2.2. Regression model predicts ccRCC grades as accurately as classification model with fewer prediction errors

DenseNet-121 and Inception-v3, the CNN models widely used for pathological image analyses [30,32–34], were employed to examine the generality of the results across the model architectures. The effectiveness of fine-tuning for developing histopathological deep-learning models was reported [35,36]. Models at the epoch of the least mean validation loss, *i.e.* DenseNet-121 at epoch 48 (regression and classification) and Inception-v3 at epoch 47 (regression) and 44 (classification) were adopted for further analyses for the highest predictive performance (Supplementary Fig. 1).

The root mean square error (RMSE) of the predictions made by the DenseNet-121 and Inception-v3 regression models were 0.116 and 0.125, respectively. Astonishingly, the distributions of the predictions showed sharp peaks at the actual grades (Fig. 2a). This result confirmed that the regression models successfully captured the histopathological grading of ccRCC, and showed that the predictions of the regression models were robust to the micro variations within the images of each grade. The *k*-means clustering on the predictions of the regression models (in continuous values) split them into four classes corresponding to G1 through G4 (Fig. 2b). Multiple attempts of clustering confirmed that its results were stable. The categorical predictions converted thus resulted in a high overall accuracy of 0.990 (DenseNet-121) and 0.985 (Inception-v3) (Fig. 2c–Table 2). These values were comparable to those of the classification CNN models: 0.989 (DenseNet-121) and 0.995 (Inception-v3) (Fig. 2d–Table 2). This result shows that the predictive performance of the regression models was equivalent to that of the commonly used classification models on the four-class grading of ccRCC. The result further suggests that a clustering algorithm as simple as *k*-means clustering is sufficient to convert the predictions of the regression models to categorical predictions. The same tendency shown by the two CNN models verifies the generality of this argument among the CNN architectures.

A careful comparison of the predictions identified that the regression models made fewer critical prediction errors, where predicted and the actual grades differed by more than one grade (a G2 sample predicted as G4, for instance) (Fig. 2c and d). This tendency was distinct in DenseNet-121; the regression models made one critical error (0.020% of the samples), whereas the classification models made 14 critical errors (0.28% of the samples). We found that the majority of the critical mispredictions, especially G1 and G2 as G4, happened when there was a nontrivial portion of non-carcinoma tissues (Supplementary Fig. 2). This result implies that the presence of the non-carcinoma tissue in the patch is the necessary condition for such mispredictions and that both regression and classification models cannot exert their predictive ability well on such samples. It should be emphasized that, in practice, a few mispredictions are virtually negligible, because the predictions

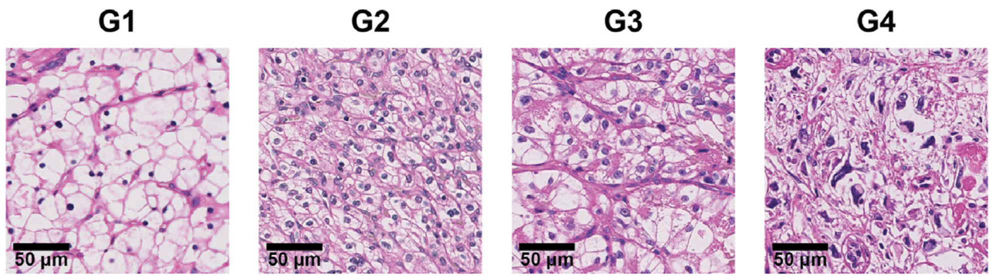

Fig. 1. Representative image patches of each grade.

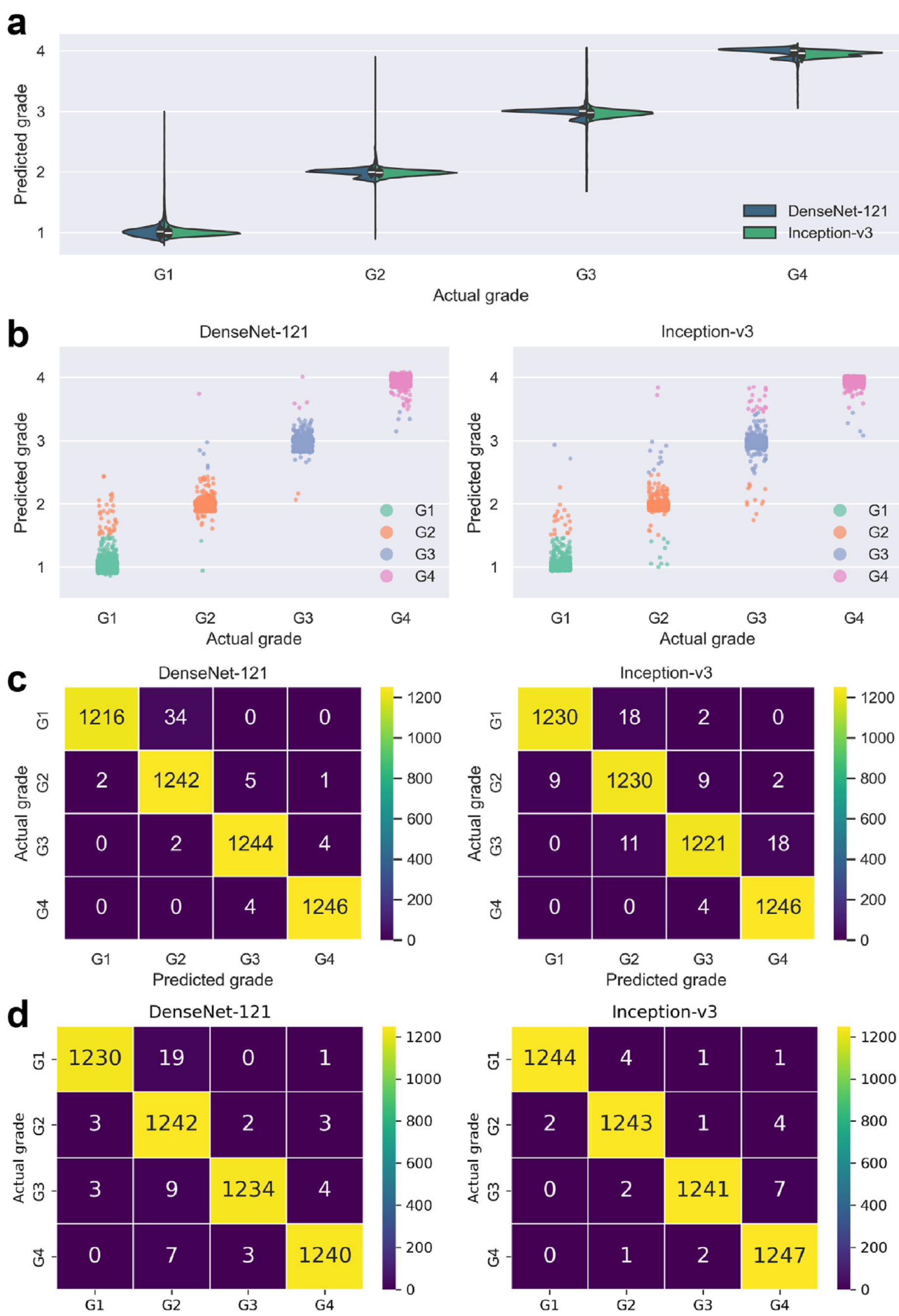

Fig. 2. The regression models vs. classification models on the four-grade prediction. (a) Violin plot of the predictions of the regression models. (b) Jitter plot of the predictions of the regression models colored by the predicted classes. (c, d) Confusion matrix on the predictions of the regression (c) and classification (d) models.

Table 2
The accuracy of the classification and regression models on the four-grade prediction.

WHO/ISUP grade	Classification: DenseNet-121	Classification: Inception-v3	Regression: DenseNet-121	Regression: Inception-v3
G1	0.984	0.995	0.973	0.984
G2	0.994	0.994	0.994	0.984
G3	0.987	0.993	0.995	0.977
G4	0.992	0.998	0.997	0.997
Overall	0.989	0.995	0.990	0.985

are given based on the distribution of the multiple patches cropped from the WSIs. Nevertheless, the methods to prevent such critical mispredictions are worth considering to enhance model reliability. Restricting the input images to those entirely covered by carcinoma regions and adopting machine learning models to filter out image patches with non-carcinoma tissue are two possible countermeasures. The fewer critical errors of the regression models are considered to be rooted in the maintenance of the relationships

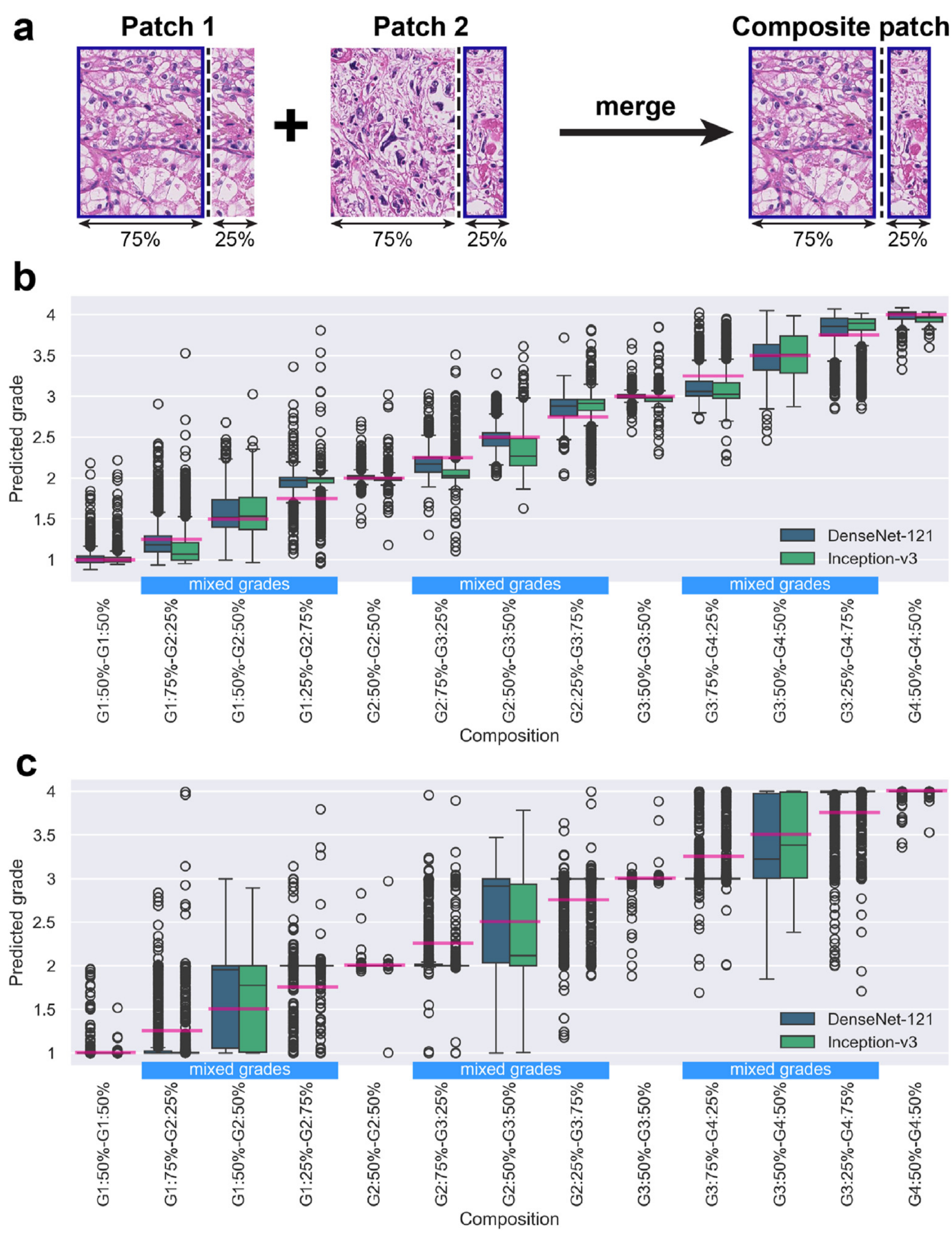

Fig. 3. Grade predictions of the regression models on the composite images mimicking the grade ITH. (a) An example of the composite images. The segments of the two images (in navy boxes) were merged to yield a composite image. (b, c) The box plot of the grades predicted by the regression (b) and the classification (c) models. The pink line shows the expected grades.

among the ccRCC grades, *i.e.* carcinoma of a grade (*e.g.* G2) is more similar to that of a neighboring grade (*e.g.* G1, G3) than non-neighboring grade (G4). This information is lost in the one-vs-rest multi-class classification, as it reduces the four grades (G1 to G4) to the binary classes (grade of interest or not). The critical errors must be minimized, if not none, for the machine learning models to make reliable supportive tools of carcinoma grading in practice. Our results show a strong advantage of the regression models over the classification models in the context of being adopted for the practical carcinoma grade prediction tools.

2.3. Regression CNN models can detect the grade ITH of ccRCC

As a proof-of-concept study, we prepared hypothetical ITH image patches and made our regression and classification models predict their grades. The hypothetical ITH patches were generated by concatenating the segments of the two patches at different ratios (Fig. 3a, see MATERIALS AND METHODS section for details). These composite images were considered the simplest mimic of the grade heterogeneity where carcinomas of different grades coexist locally. To allow flexible expression of the ccRCC grades, we extended the definition of the grades from the classical four integers (1, 2, 3, and 4) to allow decimal. The grades of the composite images were calculated as the weighted average of the grades of the source patches, where the proportions of the segments were treated as the weights (Supplementary Table 1, pink line in Fig. 3b and c). The predictions of the classification models were computed as the expected values of the grade using the computed probabilities of the image belonging to each grade.

To ensure that the procedure of combining images did not affect the grade predictions, the composite images were made from the patches of identical grades. Both for the regression and classification models, the center of the predictions on these images agreed well with the expected grades of the images (Supplementary Fig. 3). This result confirmed that the merge of the patch segments did not influence the predictions of our CNN models. In the regression models, a linear-like relationship was found between the center of the prediction distributions and the expected grades of the composite images made from two different grades (Fig. 3b). Remember that the CNN models were only trained with the classical four-grade data. This observation validates our flexible grade expression and suggests that the regression CNN models can predict grades reflecting the grade heterogeneity within a single image patch. This tendency was absent for the classification models (Fig. 3c). In classification models, the grade predictions were inclined towards the more populating grade (in case of 25%–75% composition) or spread between the two grades of the source patches (in case of 50%–50% composition). This result demonstrates that the classification models tend to advocate one class over the others in grade prediction and are insensitive to grade heterogeneity. Our analysis revealed that the regression CNN models can detect grade ITH by allowing continuous grade expression.

3. Conclusion

We examined the applicability of the regression CNN models for predicting the histological grade of carcinoma using ccRCC as an example. Our study revealed that the regression models can classify carcinoma grades as accurately as the classification models with enhanced prediction reliability. This feature equips the regression models with a strong advantage over the classification models when implemented in the practical supportive tools for carcinoma grading, where such errors must be minimized. We further investigated the sensitivity of the regression models to ITH using mixed-grade images as a proof of concept. Our results showed that the raw predictions of the regression models roughly reproduced the expected grades of the composite images, suggesting that the regression CNN models can detect ITH. This feature was absent in the classification models. Our findings suggest that the regression models should be sufficiently compatible with the classification models with the additional advantages of i) making fewer critical prediction errors and ii) detecting ITH, for the histological four-class grading of ccRCC. Examining the generality of our findings with other types of cancers is one indispensable direction for future studies. This work will stimulate further studies of the regression machine learning models on multi-class carcinoma grading and ITH detection to develop practically supportive tools for medical practitioners, enabling more efficient and accurate carcinoma gradings.

4. Materials and methods

4.1. Ethics

One hundred and twenty-five patients who underwent radical nephroureterectomy (RNU) for ccRCC at Keio University Hospital between 2000 and 2017 were identified. Tissue samples were obtained from consenting patients in the present study, which was approved by the Ethics Committee of Keio University (ethical committee number: 20200189) and National Center for Child Health and Development Research Institute (ethical committee number: 2020–196). All specimens were fixed in 10% formalin and embedded in paraffin, and all hematoxylin and eosin-stained slides were reviewed by a genitourinary pathologist (board-certified pathologist, S.M., with 34 years of experience in pathology). The WSIs were taken using NanoZoomer digital pathological image (Hamamatsu Photonics) magnified by a factor of 20.

4.2. Image patches

The WSIs of uniform grade were selected. From the WSIs, patches of 435 pixels by 439 pixels (approximately 200 μm square) were randomly cropped from the manually annotated carcinoma region. The number of patches was determined to be proportional to the area of the carcinoma region (1 patch/1,333 μm^2). The pathologist (M.N., more than 30 years of experience) discarded the patches of non-carcinoma tissue, ungradable carcinoma tissue, and wide background. The grades of the patches followed those of the WSIs diagnosed by S.M. based on WHO/ISUP grading guidelines [21,22]. Patches of G3 and G4 were augmented by PyTorch [37] to abound training data for the CNN models. Here, the following techniques were randomly applied: horizontal flip, vertical flip, rotation, posterization, grayscale, color jitter (on brightness, contrast, saturation, hue), and partial erasing. The composite images mimicking the grade ITH were made by concatenating the segments of the two image patches from G1 to G4 in a randomly determined pair except for the combinations between the grades of which the discrepancy was greater than one. Two images were combined at the proportion of either 25% or 50% and the expected grades for the composite images were computed as the mean of the grades considering the proportion. For each composition, 250 composite images were prepared.

4.3. CNN models

The CNN models for ccRCC grade prediction were developed from DenseNet-121 [38] and Inception-v3 [39] trained on ImageNet-1K dataset using fine-tuning. The number of nodes in the final fully connected layer was replaced to one (regression models) or four (classification models). Parameters in all the layers were optimized to the ccRCC images using Adam [40] as the optimizer until 50 epochs under the batch size of 64. Cross-validation was performed five times to evaluate the performance of our models. A model was trained and validated for each trial with 10,000 (2,500 patches per grade) and 1,000 (250 patches per grade) image patches, respectively. After the validation images were separated from the whole dataset, training samples were randomly selected from the remaining images. If the remaining images were insufficient to make 2,500 training images per grade, augmented images of that grade were added to the training dataset. It should be noted that validation images did not overlap among the trials. The best-performing CNN models were identified as those at the epoch with the least mean validation loss in the five trials. The predictions of the regression model (grade in continuous values) were converted to the categorial classes by k-means clustering ($n_{\text{clusters}} = 4$) on all the predictions using scikit-learn [41]. The accuracy was computed from all the predictions made in the five trials. The grades of the composite images were predicted by the best-performing CNN models. Note that there was no overlap in the training and source patches of the composite images. The models were developed and managed using PyTorch.

4.4. Web application

Python CGI for grade predictions of the regression CNN models was developed and is available at Docker Hub (https://hub.docker.com/r/mayushibata/rcc) as a Docker container [42].

Data availability

The image patches and the CNN models are available upon request.

Author contributions

A. U. conceived the study. M.O., R.M., and S.M. handled the ethics. S.M., M.N., S.A., and M.S. performed data collection and preprocessing. M.S. developed the models. M.S., S.A., K.O., and A.U. designed the experiments and participated in discussions. S.M., K.Y., M.O., and R.M. provided feedback. All authors prepared the manuscript.

Declaration of Generative AI and AI-assisted technologies in the writing process

During the preparation of this work the authors used DeepL, ChatGPT, and Grammerly for English writing. After using these tools/services, the authors reviewed and edited the content as needed and take full responsibility for the content of the publication.

Funding

This work was supported by JSPS KAKENHI Grant Number JP23K20315 and the Grant of National Center for Child Health and Development.

Declaration of competing interest

None declared.

Acknowledgments

The authors thank Motohiro Kuriyama for cropping the image patches. The computation was conducted on the cluster of HPE ProLiant DL360 Gen 10 at National Center for Child Health and Development Research Institute, and on Chaen, the supercomputer of the Center for Interdisciplinary AI and Data Science at Ochanomizu University.

Appendix A. Supplementary data

Supplementary data to this article can be found online at https://doi.org/10.1016/j.reth.2025.01.011.

References

[1] Elazab N, Gab-Allah WA, Elmogy M. A multi-class brain tumor grading system based on histopathological images using a hybrid YOLO and RESNET networks. Sci Rep 2024;14:4584.
[2] Sajjad M, Khan S, Muhammad K, Wu W, Ullah A, Baik SW. Multi-grade brain tumor classification using deep CNN with extensive data augmentation. J Comput Sci 2019;30:174–82.
[3] Abdelli A., Saouli R., Djemal K., Youkana I. Combined datasets for breast cancer grading based on multi-CNN architectures. in 2020 tenth international conference on image processing theory, tools and applications (IPTA). 1-7 (IEEE).
[4] Voon W, Hum YC, Tee YK, Yap WS, Salim MIM, Tan TS, et al. Performance analysis of seven Convolutional Neural Networks (CNNs) with transfer learning for Invasive Ductal Carcinoma (IDC) grading in breast histopathological images. Sci Rep 2022;12:19200.
[5] Kumaraswamy E, Kumar S, Sharma M. An invasive ductal carcinomas breast cancer grade classification using an ensemble of convolutional neural networks. Diagnostics 2023;13:1977.
[6] Lucas M, Jansen I, Savci-Heijink CD, Meijer SL, de Boer OJ, van Leeuwen TG, et al. Deep learning for automatic Gleason pattern classification for grade group determination of prostate biopsies. Virchows Arch 2019;475:77–83.
[7] Karimi D, Nir G, Fazli L, Black PC, Goldenberg L, Salcudean SE. Deep learning-based gleason grading of prostate cancer from histopathology images - role of multiscale decision aggregation and data augmentation. IEEE J Biomed Health Inform 2019;24:1413–26.
[8] Jones AD, Graff JP, Darrow M, Borowsky A, Olson KA, Gandour-Edwards R, et al. Impact of pre-analytical variables on deep learning accuracy in histopathology. Histopathology 2019;75:39–53.
[9] Mehra R. Breast cancer histology images classification: training from scratch or transfer learning? ICT Express 2018;4:247–54.
[10] Tian K, Rubadue CA, Lin DI, Veta M, Pyle ME, Irshad H, et al. Automated clear cell renal carcinoma grade classification with prognostic significance. PLoS One 2019;14:e0222641.
[11] Musulin J, Štifanić D, Zulijani A, Ćabov T, Dekanić A, Car Z. An enhanced histopathology analysis: an AI-based system for multiclass grading of oral squamous cell carcinoma and segmenting of epithelial and stromal tissue. Cancers 2021;13:1784.
[12] Linkon AHM, Labib MM, Hasan T, Hossain M. Deep learning in prostate cancer diagnosis and Gleason grading in histopathology images: an extensive study. Inform Med Unlocked 2021;24:100582.
[13] Galar M, Fernández A, Barrenechea E, Bustince H, Herrera F. An overview of ensemble methods for binary classifiers in multi-class problems: experimental study on one-vs-one and one-vs-all schemes. Pattern Recogn 2011;44:1761–76.
[14] Ramón y Cajal S, Sesé M, Capdevila C, Aasen T, De Mattos-Arruda L, Diaz-Cano SJ, et al. Clinical implications of intratumor heterogeneity: challenges and opportunities. J Mol Med 2020;98:161–77.
[15] Zhang D, Ni Y, Wang Y, Feng J, Zhuang N, Li J, et al. Spatial heterogeneity of tumor microenvironment influences the prognosis of clear cell renal cell carcinoma. J Transl Med 2023;21:489.
[16] Hsieh JJ, Purdue MP, Signoretti S, Swanton C, Albiges L, Schmidinger M, et al. Renal cell carcinoma. Nat Rev Dis Prim 2017;3:1–19.
[17] Muglia VF, Prando A. Renal cell carcinoma: histological classification and correlation with imaging findings. Radiol Bras 2015;48:166–74.
[18] Ljungberg B, Hanbury DC, Kuczyk MA, Merseburger AS, Mulders PF, Patard JJ, et al. Renal cell carcinoma guideline. Eur Urol 2007;51:1502–10.
[19] Cheville JC, Lohse CM, Zincke H, Weaver AL, Blute ML. Comparisons of outcome and prognostic features among histologic subtypes of renal cell carcinoma. Am J Surg Pathol 2003;27:612–24.
[20] Teloken PE, Thompson RH, Tickoo SK, Cronin A, Savage C, Reuter VE, et al. Prognostic impact of histological subtype on surgically treated localized renal cell carcinoma. J Urol 2009;182:2132–6.
[21] Delahunt B, Cheville JC, Martignoni G, Humphrey PA, Magi-Galluzzi C, McKenney J, et al. The International Society of Urological Pathology (ISUP) grading system for renal cell carcinoma and other prognostic parameters. Am J Surg Pathol 2013;37:1490–504.
[22] Delahunt B, Sika-Paotonu D, Bethwaite PB, Jordan TW, Magi-Galluzzi C, Zhou M, et al. Grading of clear cell renal cell carcinoma should be based on nucleolar prominence. Am J Surg Pathol 2011;35:1134–9.
[23] Dagher J, Delahunt B, Rioux-Leclercq N, Egevad L, Srigley JR, Coughlin G, et al. Clear cell renal cell carcinoma: validation of World Health organization/

international society of urological pathology grading. Histopathology 2017;71:918–25.
[24] Gerlinger M, Horswell S, Larkin J, Rowan AJ, Salm MP, Varela I, et al. Genomic architecture and evolution of clear cell renal cell carcinomas defined by multiregion sequencing. Nat Genet 2014;46:225–33.
[25] Manini C, López-Fernández E, López JI. Towards personalized sampling in clear cell renal cell carcinomas. Cancers 2022;14:3381.
[26] Li Y, Lih TSM, Dhanasekaran SM, Mannan R, Chen L, Cieslik M, et al. Histopathologic and proteogenomic heterogeneity reveals features of clear cell renal cell carcinoma aggressiveness. Cancer Cell 2023;41:139–163.e17.
[27] López JI. Intratumor heterogeneity in clear cell renal cell carcinoma: a review for the practicing pathologist. APMIS 2016;124:153–9.
[28] Lopez JI, Angulo JC. Pathological bases and clinical impact of intratumor heterogeneity in clear cell renal cell carcinoma. Curr Urol Rep 2018;19:1–7.
[29] Roy K, Banik D, Bhattacharjee D, Nasipuri M. Patch-based system for classification of breast histology images using deep learning. Comput Med Imaging Graphics 2019;71:90–103.
[30] Barsha NA, Rahman A, Mahdy M. Automated detection and grading of invasive ductal carcinoma breast cancer using ensemble of deep learning models. Comput Biol Med 2021;139:104931.
[31] Kott O, Linsley D, Amin A, Karagounis A, Jeffers C, Golijanin. D. et al. Development of a deep learning algorithm for the histopathologic diagnosis and Gleason grading of prostate cancer biopsies: a pilot study. Eur Urol Focus 2021;7:347–51.
[32] Riasatian A, Babaie M, Maleki D, Kalra S, Valipour M, Hemati S, et al. Fine-tuning and training of densenet for histopathology image representation using TCGA diagnostic slides. Med Image Anal 2021;70:102032.
[33] Buddhavarapu VG. An experimental study on classification of thyroid histopathology images using transfer learning. Pattern Recognit Lett 2020;140:1–9.
[34] Ahmed S, Shaikh A, Alshahrani H, Alghamdi A, Alrizq M, Baber J, et al. Transfer learning approach for classification of histopathology whole slide images. Sensors 2021;21:5361.
[35] Mahbod, A., Ellinger, I., Ecker, R., Smedby, Ö., Wang, C. Breast cancer histological image classification using fine-tuned deep network fusion. in Image Analysis and Recognition: 15th International Conference, ICIAR 2018, Póvoa de Varzim, Portugal, June 27-29, 2018, Proceedings 15. 754-762 (Springer).
[36] Kandel I, Castelli M. How deeply to fine-tune a convolutional neural network: a case study using a histopathology dataset. Appl Sci 2020;10:3359.
[37] Paszke A, Gross S, Massa F, Lerer A, Bradbury J, Chanan G, et al. Pytorch: an imperative style, high-performance deep learning library. Adv Neural Inf Process Syst 2019:32.
[38] Huang G, Liu Z, van der Maaten L, Weinberger KQ. Densely connected convolutional netoworks. Preprint at, https://arxiv.org/abs/1608.06993; 2016.
[39] Szegedy C, Vanhoucke V, Ioffe S, Shlens J, Wonja Z. Rethinking the Inception architecture for computer vision. Preprint at, https://arxiv.org/abs/1512.00567; 2015.
[40] Kingma DP, Ba J. Adam: a method for stochastic optimization. Preprint at, https://arxiv.org/abs/1412.6980; 2014.
[41] Pedregosa F, Varoquaux G, Gramfort A, Michel V, Thirion B, Grisel O, et al. Scikit-learn: machine learning in Python. J Mach Learn Res 2011;12:2825–30.
[42] Merkel D. Docker: lightweight linux containers for consistent development and deployment. Linux J 2014;239:2.